Enhancing mechanical properties of glass ionomer cements with basalt fibers

Xiaozhen Bao[1], Sufyan Garoushi[2], Fang Liu[1], Lippo L.J. Lassila[2], Pekka K. Vallittu[2,3], Jingwei He[1,2,*]

[1] College of Materials Science and Engineering, South China University of Technology, Guangzhou, China

[2] Department of Biomaterials Science and Turku Clinical Biomaterials Center-TCBC, Institute of Dentistry, University of Turku, Turku, Finland

[3] City of Turku Welfare Division, Oral Health Care, Turku, Finland

* Corresponding Author: Jingwei He, Email: msjwhe@scut.edu.cn

1. Introduction

As a promising dental restorative material, glass ionomer cements (GICs) are widely used in many dental applications such as defect repair, cavity filling, lining, pit and fissure sealing, and so on [1,2]. Distinguished from resin composites, GICs have several advantages, such as biocompatibility, lower pulp irritation, effective chemical adhesion to dentin and enamel, similar thermal expansion coefficient as tooth structure, and low microleakage [3-5]. Moreover, GICs can promote the remineralization of tooth structure and prevent secondary caries due to the constant release of fluoride ions and the ability to absorb fluoride ions from fluoride toothpaste and fluoride mouthwash [6]. However, GICs could not completely replace resin composites in dentistry to the extent that mechanical properties of GICs are far less than that of resin composites [7].

In recent years, researchers have done a lot of researches on improving the mechanical properties of GICs, and found that nano-TiO2 [8, 9], chitosan [10, 11], cellulose fibers [12], hydroxyapatite [13], and glass fibers [14] could be used in GICs to improve its mechanical properties. Among them, the reinforcing effect of glass fibers is particularly remarkable. This should be attributed to the fact that the short glass fibers are effective in preventing the propagation of cracks in matrix. Garoushi *et al*., [15] found that adding 25 wt. % of glass fibers with 200-300 μm in length could significantly increase flexural strength and diametral tensile strength of GICs, but continue adding would cause the decrease of tested mechanical properties. Hammouda *et al*., [14] incorporated 3 wt.% and 5 wt.% of 1 mm glass fibers into GICs, and found that glass fibers could greatly improve diametral tensile strength, flexural strength, surface hardness, and fracture toughness of GICs.

The chemical composition of basalt fibers is similar to that of glass fibers [16], but the production process of basalt fibers is more environmentally friendly and energy-saving than glass fibers and they can automatically convert into soil medium after being discarded [17, 18].

Basalt fibers also have better chemical stability because of the excellent acid-, alkali- and water resistance [19]. Tensile strength of basalt fibers is generally between that of E-glass fiber and S-glass fiber [20], and it can even exceed S-glass fiber if excellent production technics and proper chemical compositions and mineral components are adopted [21,22]. When used as reinforcing filler, basalt fibers showed stronger interfacial adhesion with various resins than glass fibers [17, 23, 24], and were proven to have excellent reinforcement for thermoplastics and thermosets [25-27]. Furthermore, basalt fibers are nontoxic to human beings due to its chemical inertness [28].

To our knowledge, there is no research concerned about enhancement of GICs by basalt fibers, hence the study was taken to evaluate the enhancement effects of basalt fibers on mechanical properties of GICs, and the fiber length as well as addition amount of basalt fibers were chosen as two important factors.

2. Materials and Methods

2.1 Preparation of basalt fibers reinforced GICs specimens

The continuous basalt fibers (BF, *Φ*13.3 μm) were cut into 1 mm and 2 mm, and then were added into glass powders (fluoroaluminosilicate glass) of commercial self-cure GICs (GC Fuji IX, Jiangsu, Japan) with a series of mass fraction (3wt.%, 5wt.%, 7wt.%, and 9wt.%) and hand-mixed until a homogenous mixture was obtained. The BF contained glass powders were then mixed with cement liquid (modified polyacrylic acid & water) at a powder/liquid (P/L) mass ratio of 3.6g /1g at room temperature according to the product description. After that, the mixed paste was quickly filled into mold with specific sizes according to different measurements. Polyester film was used as covering and appropriate force was applied to ensure that the paste was filled into the mold adequately and the air bubbles were removed. After ten minutes, the cured specimen was removed out of the mold and kept dry for one hour at 37℃, then transferred into deionized water and stored at 37℃ for a certain time according to different measurement. The specimens of commercial GICs without basalt fibers were also prepared in the same way as control group. All specimens had to be polished using 600 grit sand papers before testing by a metallographic polishing machine (MDP-1, Shanghai guangxiang sample preparation equipment Int., China).

2.2 Measurement of mechanical properties

All mechanical properties tests were performed on a universal testing machine (AGS-10KNI, Shimadzu, Japan) with a crosshead speed of 1 mm/min for three point bending and fracture toughness (FT) tests, 0.75 mm/min for compress strength (CS) test. Eight samples (n=8) of every group were prepared for each test. The specimens were prepared in a silicone mold sized 2 mm × 2 mm × 25 mm for three-point bending test, in a silicone mold sized *Φ* 6 mm × 4 mm for CS test, and in a Teflon mold sized 5 mm × 2 mm × 25 mm with a 2.5 mm notch in the middle of the mold for FT test.

FS and FM were obtained by three-point bending test with a test span of 20 mm and were calculated by the equations as follows:

$$FS=3PL/(2bh^2)$$

$$FM=SL^3/(4bh^3)$$

Where P is the maximum load, L is the span length (20 mm), b is the width of the specimen and h is the thickness of the specimen. S is the stiffness (N/m). S=F/d and d is the deflection corresponding to load F at a point in the straight-line portion of the trace.

CS was calculated as follows:

$$CS=P/(\pi r^2)$$

Where *P* is the maximum load, r is the radius of cylinder-shaped specimen.

FT was calculated as K_{IC} according to following equation:

$$K_{IC}=\frac{3Pl}{2BW^{3/2}}f(a/W)$$

Where f (a/W) = $[1.93(a/W)^{0.5}-3.07(a/W)^{1.5}+14.53(a/W)^{2.5}-25.11(a/W)^{3.5}+25.8(a/W)^{4.5}]$, *P* is the maximum load, *l* is the span length, B is the thickness of specimen, W is the width of the specimen, and a is the notch length.

2.3 Measurement of length distribution of fibers

0.2 g of 1 mm and 2 mm cut BF were put into two glass petri dishes, respectively, and then dispersed as evenly as possible using a slender tool. The BF were photographed with polarizing microscope (BX51-P LINKAMTHMS600, Guangzhou, Japan) at a magnification of 50×. The actual lengths of 1000 fibers for each size of BF were obtained using Image-J processing program.

2.4 Measurement of water sorption (WS) and solubility (SL)

Wafer-shaped specimens (*Φ*15 mm × 2 mm) of GIC with 7 wt. % of 2 mm BF fibers and control GIC were prepared and dried to constant weight in an vacuum oven (BPZ-6063, Shanghai, China) at 80℃. The weight (m_0) of each dry specimen was measured by an analytical balance (FA1104J, Shanghai, China) with an accuracy of 0.1 mg. The specimens (n=5) were then immersed in 40 mL of deionized water at 37℃ for fixed time intervals (1 day, 1 week, 2 weeks, 3 weeks and 1 month). The specimens were taken out at the set time and lightly dried with filter paper and weighed to get m_1. Then, they were dried at 80℃ in vacuum oven until reaching constant weight and recorded as m_2. Water sorption (WS) and solubility (SL) were calculated using the following equations:

$$WS=\frac{m_1-m_2}{m_0} \times 100\%$$

$$SL=\frac{m_0-m_2}{m_0} \times 100\%$$

2.5 Water aging experiment

Compared with CS test, three-point bending test and FT test can better reflect mechanical properties of brittle materials such as GICs, and the results obtained from FT test were often consistence with the results obtained from three-point bending test [2,15]. Therefore, the aging properties were investigated by the variation in FS and FM after water immersion. According to the results of mechanical tests, optimal BF reinforced GIC with 7 wt.% of 2 mm fibers was chosen for water aging experiment, and GIC without fibers was used as control. Six groups (n=8) of each experimental GICs were immersed in water at 37℃ for 1 day, 1week, 2 weeks, 1 month, 2 months and 3 months, respectively. The results of FS and FM after water immersion were obtained according to the same method as mentioned above.

2.6 Microscopic analysis

BF were mixed with GIC liquid and stored at 37℃ for one hour. Then, the BF-liquid mixture was extracted in tetrahydrofuran by Soxhlet extractor for 72 hours, and obtained BF were dried at 60℃ until getting constant weight (BF without liquid mixing were treated in the same way as control). Microscopic photographs of BF as well as fraction surface and side surface of experimental GICs for three-point bending test were taken by a scanning electron microscopy (EV018, Carl zeiss AG, Germany) after platinization.

2.7 Statistical analysis

The results of FS, FM, FT and CS were statistically analyzed by SPSS 17.0 (SPSS 17.0, IBM Corp., USA) with analysis of variance (ANOVA) at the $p<0.05$ significance level. Subsequent multiple comparisons were conducted using Tukey's *post hoc* analysis.

3. Results

The results of FS, FM, CS and FT of experimental GICs were summarized in Table 1. It was obvious that BF with appropriate fiber length and mass fraction can significantly improve the mechanical properties of commercial GICs (p<0.05). Regardless of the fiber length, FS increased as the mass fraction of BF increased. Incorporation of 7 wt.% and 9 wt.% of BF could improve FS of GICs significantly (p<0.05). However, for FM and CS, there was no obvious correlation between value and fibers mass fraction. Compared with control group, FT of experimental GICs were significantly increased (p<0.05). With the same mass fraction, the fibers length had no significant influence on FT (p>0.05) except for GICs with 9 wt.% of BF, GIC with 2 mm BF had higher FT than GIC with 1 mm BF (p<0.05).

According to Table 2, the effects of water aging time on FS of control GIC and BF reinforced GIC were not the same. For control GIC, FS had no significant variation during the first two months (p>0.05), and even increased (p<0.05) after being immersed in water for 3 months. For BF reinforced GIC, FS kept decreasing during the first month's immersion (p<0.05), and became stable after one month (p>0.05). The FS of BF reinforced GIC were higher (p<0.05) than that of control GIC in the first two weeks' immersion, and became comparable (p>0.05) with FS of control GIC after that immersion time. However, water aging time had no influence on FM of experimental GICs (p>0.05), and FM of experimental GICs were the same with each other (p>0.05) in all time intervals.

Figure 1 illustrated stress-extension curves of BF reinforced GIC and control GIC. Control GIC showed apparent brittleness whereas BF reinforced GICs revealed high toughness (energy from preload to maximum extension); exhibiting stable crack propagation, while specimens without fiber reinforcement failed in a catastrophic manner.

The results of water sorption and solubility of experimental GICs at the aging time were shown in Table 3. It was clear that water sorption of BF reinforced GIC was higher than control

GIC (p<0.05). BF reinforced GIC had comparable solubility as control GIC (p>0.05) at all time intervals, except for sample with 3 weeks of immersion, which showed higher solubility than control GIC (p<0.05).

Microscope photos of 1 mm BF and 2 mm BF were shown in Figure 2, and length distribution of them were demonstrated in Figure 3 and Figure 4, respectively. From Figure 3 and Figure 4, it could be seen that length of 1 mm cut BF fibers were mainly distributed in the range of 1.0 mm to 1.4 mm, and length of 2 mm cut BF fibers were mainly distributed in the range of 1.9 mm to 2.3 mm.

The SEM photos of fracture surface and side surface of three-point bending samples were shown in Figure 5. There were lots of cracks could be observed on the side surface of BF reinforced GIC (Figure 5b), and on the fracture surface of BF reinforced GIC, there existed pull-out and random orientated basalt fibers (Figure 5d). The SEM photos of extracted BF and cement liquid-treated BF were shown in Figure 6. It could be observed that the surface of untreated BF was smoother than cement liquid-treated BF.

4. Discussion

The Purpose of this study was to improve the mechanical properties of GICs using BF fibers. As can be seen from Table 1, introducing BF could achieve a great improvement in mechanical properties of control GIC as desired. Within a certain range, the longer the fibers length and the more the fibers added, the better the reinforcing effect. It was similar to the modification effects of glass fiber on GICs [14, 29]. However, if the fibers were too long, it's not beneficial for mixing fibers and glass powders together uniformly, and excessive addition of BF may cause handling problem [2]. Both of these two situations would induce reduction of mechanical properties, thus appropriate length and mass fraction of fibers were important for obtaining high mechanical properties. In this study, based on the results of FS, FM, FT and CS, it seemed that 2 mm BF had better reinforcement effect on GIC than 1 mm BF, and 7 wt.% was the optimal mass fraction of 2 mm BF, for 9 wt.% of BF had already made it hard to prepare samples. Therefore, GIC reinforced with 7 wt. % of 2 mm BF were used for water aging experiments.

The stress-extension curves in Figure 1 indicated that complete destruction of BF reinforced GICs specimen required more fracture energy, confirming the unquestionable enhancement effect of BF. Hence, incorporation of discontinuous BF to a GIC matrix increases the toughening mechanism known as "crack bridging", which occurs when the crack surfaces are pulled together by the reinforcing phase, demanding extra energy for the crack tip to propagate further [2].

The SEM photos in Figure 5 showed that, before three-point bending testing, the specimen of BF reinforced GIC had several obvious cracks on the side surface (Fig.5 (b)), while it was hard to notice cracks on the side surface of control GIC (Fig.5 (a)). Usually, fiber reinforced GIC needs more liquid than unmodified GIC, but in this research, mass ratio of cement liquid was kept the same, thus drying cracks occurred in BF reinforced GIC. After three point bending test, the side surface of control GIC was still looked smooth, but more cracks appeared on the

side surface of BF reinforced GIC. The fracture surface photograph of BF reinforced GIC provided information that cracks propagated from GIC matrix to BF, this meant that introducing BF could resist the fracture crack propagation by transferring stresses from GIC matrix to BF, changing the direction of crack propagation and preventing matrix from continuing destruction [14,15,30]. More cracks would consume more energy, so more energy should be applied to cause complete fracture of BF reinforced GIC when compared with control GIC, this was consistence with the result showed in Figure 1. The SEM photos of cement liquid-treated BF showed a certain chemical interaction between fiber and cement liquid, similar to the acid-base interaction between glass powder and liquid, which improved the adhesion of fiber to matrix and was beneficial for mechanical properties. However, according to the fracture surface photograph of BF reinforced GIC, the main damage modes were fibers pull-out and debonding, moreover, there were gaps between GIC matrix and basalt fibers, and little contact could be found. It might be due to that the original adhesion between fibers and matrix was poor, which could be damaged by water erosion and mechanical stress.

GIC is a brittle material and has a tensile strength that is markedly lower than its compressive strength. This material fails by crack propagation that is favored by tensile rather than compressive loading. Flexural strength, flexural modulus, and fracture toughness test the material under both compressive and tensile loading [31]. Dowling *et al*., demonstrated the validity of the three-point bending test for measuring GICs strengths (FS, FM, FT) in comparison with compression testing which they claimed it was not valid for predicting the performance of GICs [32]. In general, the effect of discontinuous fiber reinforcement on the fracture toughness and flexural properties tests were observable and more obvious than in the compression test, where fibers were oriented most likely in the same load direction [33]. It has been shown early on that fiber orientation is an important factor influencing the mechanical properties of fiber reinforced composite [34].

Water plays an important role in the setting process of GICs [35,36]. Firstly, it was the medium through which the acid-base reaction could proceed [37]; Secondly, it could destroy the carboxylate structure formed during the acid-base reaction process [38], thus the carboxylate structure was always in the formation-hydrolysis dynamic balance process. In other word, properties of GICs might be variation all the time in a moisture environment just like in the oral cavity. Therefore, the aging characteristic of GICs in water was investigated in is study, including variation of FS, FM, water sorption, and solubility with aging time.

It was noticed that water sorption of BF reinforced GIC were always higher than control GIC during testing time. This might be due to three reasons: the first was the poor impregnation of BF in GIC matrix, which would result in small crevices between matrix and BF [15], and the crevices allowed the BF reinforced GIC to have potential to store more water; the second was the adhesion between BF and matrix, even though BF had some interaction with cement liquid as shown in Figure 6, but this interaction might be not strong enough and sensitive to water, leading to microleakage between BF and matrix after water immersion and allowing more water to be absorbed; the third was the drying cracks as shown in Fig.5 (b) would increase the contact area between water and GIC, leading to higher water sorption.

It is well known that the mechanical properties of fiber-reinforced composites are influenced by the adhesive strength and wettability of the fibers and matrix [39,40], that's to say sufficient adhesion and wetting between BF and GICs matrix was are preconditions for transferring load from the GICs matrix to BF. In this study, FS of BF reinforced GIC gradually decreased with the increasing of aging time, but FS of control GIC was not influenced by water immersion negatively. That should be due to the interfacial adhesion between BF and matrix became worse with the prolongation of aging time, and the interfacial contacts could be released easily by local stress initiated by mechanical effects [41]. Therefore, the resistance of BF to crack

initiation and propagation at the action of load was not as good as before water immersion, leading to decrease of FS within a certain aging time.

However, the color of BF reinforced GIC was influenced by brown color of BF, did not show tooth color as control GIC. This will limit the application of BF reinforced GIC in the place where aesthetic property is required, but still be fine for lining and binder.

5. Conclusion

In conclusion, introducing BF could significantly increase the mechanical properties of GIC. However, because of the weak interaction between BF and GIC matrix, mechanical properties, water sorption and solubility of BF reinforced GICs were negatively influenced by aging in water. Therefore, further studied concerned about modifying BF surface to enhance the interaction between BF and GIC matrix should be taken.

References

[1] Fonseca R B, Branco C A, Quagliatto P S, Gonçalves L D S, Soares C J, Carlo H L, Correr-Sobrinho L. Influence of powder/liquid ratio on the radiodensity and diametral tensile strength of glass ionomer cements. Journal of Applied Oral Science, 2010, 18(6): 577-584.

[2] Garoushi S, Vallittu P, Lassila L. Hollow glass fibers in reinforcing glass ionomer cements. Dental Materials, 2017, 33(2): e86-e93.

[3] Sayyedan F S, Fathi M H, Edris H, Doostmohammadi A, Mortazavi V, Hanifi A. Effect of forsterite nanoparticles on mechanical properties of glass ionomer cements. Ceramics international, 2014, 40(7): 10743-10748.

[4] Moshaverinia A, Ansari S, Roohpour N, Reshad M, Schricker S R, Chee W W. Effects of N-vinylcaprolactam containing polyelectrolytes on hardness, fluoride release and water sorption of conventional glass ionomers. The Journal of prosthetic dentistry, 2011, 105(5): 323-331.

[5] Xie D, Brantley W A, Culbertson B M, Wang G. Mechanical properties and microstructures of glass-ionomer cements. Dental Materials, 2000, 16(2): 129-138.

[6] Munhoz T, Karpukhina N, Hill R G, Law R V. Setting of commercial glass ionomer cement Fuji IX by ^{27}Al and ^{19}F MAS-NMR. Journal of dentistry, 2010, 38(4): 325-330.

[7] Yamazaki T, Brantley W, Culbertson B, Seghi R, Schricker S. The measure of wear in N-vinyl pyrrolidinone (NVP) modifed glass-ionomer cements. Polymers for advanced technologies, 2005, 16(2-3): 113-116.

[8] Elsaka S E, Hamouda I M, Swain M V. Titanium dioxide nanoparticles addition to a conventional glass-ionomer restorative: influence on physical and antibacterial properties. Journal of dentistry, 2011, 39(9): 589-598.

[9] Garcia-Contreras R, Scougall-Vilchis R J, Contreras-Bulnes R, Kanda R, Nakajima H. Effects of TiO_2 nano glass ionomer cements against normal and cancer oral cells. In vivo, 2014, 28(5): 895-907.

[10] Petri D F S, Donegá J, Benassi A M, Bocangel J A J S. Preliminary study on chitosan modified glass ionomer restoratives. Dental materials, 2007, 23(8): 1004-1010.

[11] Kumar R S, Ravikumar N, Kavitha S, Mahalaxmi S, Jayasree R, Kumar T S S, Haneesh M. Nanochitosan modified glass ionomer cement with enhanced mechanical properties and fluoride release. International journal of biological macromolecules, 2017, 104: 1860-1865.

[12] Silva R M, Pereira F V, Mota F A P, Watanabe E, Soares S M C S, Santos M H. Dental glass ionomer cement reinforced by cellulose microfibers and cellulose nanocrystals. Materials Science and Engineering: C, 2016, 58: 389-395.

[13] Alatawi R A S, Elsayed N H, Mohamed W S. Influence of hydroxyapatite nanoparticles on the properties of glass ionomer cement. Journal of Materials Research and Technology, 2018.

[14] Hammouda I M. Reinforcement of conventional glass-ionomer restorative material with short glass fibers. Journal of the mechanical behavior of biomedical materials, 2009, 2(1): 73-81.

[15] Garoushi S K, He J, Vallittu P K, Lassila L V. Effect of discontinuous glass fibers on mechanical properties of glass ionomer cement. Acta biomaterialia odontologica Scandinavica, 2018, 4(1): 72-80.

[16] Deák T, Czigány T. Chemical composition and mechanical properties of basalt and glass fibers: A comparison. Textile Research Journal, 2009, 79(7): 645-651.

[17] Ross A. Basalt fibers: alternative to glass?. Composites Technology, 2006, 12(4).

[18] Iorio M, Santarelli M L, González-Gaitano G, González-Benito J. Surface modification and characterization of basalt fibers as potential reinforcement of concretes. Applied Surface Science, 2018, 427: 1248-1256.

[19] Manikandan V, Jappes J T W, Kumar S M S, Amuthakkannan P. Investigation of the effect of surface modifications on the mechanical properties of basalt fibre reinforced polymer composites. Composites Part B: Engineering, 2012, 43(2): 812-818.

[20] Dhand V, Mittal G, Rhee K Y, Park S J, Hui D. A short review on basalt fiber reinforced polymer composites. Composites Part B: Engineering, 2015, 73: 166-180.

[21] Novitskii A G. High-temperature heat-insulating materials based on fibers from basalt-type rock materials. Refractories and Industrial Ceramics, 2004, 45(2): 144-146.

[22] Chen X, Zhang Y, Huo H, Wu Z. Study of high tensile strength of natural continuous basalt fibers. Journal of Natural Fibers, 2018: 1-9.

[23] Wei B, Cao H, Song S. Tensile behavior contrast of basalt and glass fibers after chemical treatment. Materials & Design, 2010, 31(9): 4244-4250.

[24] Militký J, Kovačič V, Rubnerova J. Influence of thermal treatment on tensile failure of basalt fibers. Engineering Fracture Mechanics, 2002, 69(9): 1025-1033.

[25] Deák T, Czigány T, Maršálková M, Militký J. Manufacturing and testing of long basalt fiber reinforced thermoplastic matrix composites. Polymer Engineering & Science, 2010, 50(12): 2448-2456.

[26] Bashtannik P I, Kabak A I, Yakovchuk Y Y. The effect of adhesion interaction on the mechanical properties of thermoplastic basalt plastics. Mechanics of composite materials, 2003, 39(1): 85-88.

[27] Botev M, Betchev H, Bikiaris D, Panayiotou C. Mechanical properties and viscoelastic behavior of basalt fiber-reinforced polypropylene. Journal of Applied Polymer Science, 1999, 74(3): 523-531.

[28] Czigány T. Basalt fiber reinforced hybrid polymer composites//Materials Science Forum. Trans Tech Publications, 2005, 473: 59-66.

[29] Sharafeddin F, Tondari A, Alavi A A. The Effect of Adding Glass and Polyethylene Fibers on Flexural Strength of Three Types of Glass-Ionomer Cements. Res J of Biologic Scien, 2013, 8: 66-70.

[30] Li Q, Tang C, Liu F, He J. The Physiochemical Properties of Dental Resin Composites Reinforced with Milled E-glass Fibers. Silicon, 2018, 10(5): 1999-2007.

[31]. Xie D, Brantley WA, Culbertson BM, Wang G. Mechanical properties and microstructure of glass-ionomer cements. Dental Materials 2000;16:129-38.

[32]. Dowling AH, Fleming G, McGinley EL, Addison O. Improving the standard of the standard for glass ionomer: An alternative to the compressive fracture strength test for consideration. Journal of Dentistry 2012;40:189-201.

[33]. Garoushi S, Vallittu PK, Lassila L. Fracture toughness, compressive strength and load-bearing capacity of short glass fibre-reinforced composite resin. The Chinese Journal of Dental Research 2011; 14:15-24.

[34]. Dyer SR, Lassila LV, Jokinen M, Vallittu PK. Effect of fibre position and orientation on fracture load of fibre-reinforced composite. Dental Materials 2004;20:947–55.

[35] Algera T J, Kleverlaan C J, Prahl-Andersen B, Feilzer A J. The influence of environmental conditions on the material properties of setting glass-ionomer cements. Dental Materials, 2006, 22(9): 852-856.

[36] Culbertson B M. Glass-ionomer dental restoratives. Progress in Polymer Science, 2001, 26(4): 577-604.

[37] Moshaverinia A, Roohpour N, Rehman I U. Synthesis and characterization of a novel fast-set proline-derivative-containing glass ionomer cement with enhanced mechanical properties. Acta biomaterialia, 2009, 5(1): 498-507.

[38] Miyazaki M, Moore B K, Onose H. Effect of surface coatings on flexural properties of glass ionomers. European journal of oral sciences, 1996, 104(5-6): 600-604.

[39] Lee S O, Rhee K Y, Park S J. Influence of chemical surface treatment of basalt fibers on interlaminar shear strength and fracture toughness of epoxy-based composites. Journal of Industrial and Engineering Chemistry, 2015, 32: 153-156.

[40] Kobayashi M, Kon M, Miyai K, Asaoka K. Strengthening of glass-ionomer cement by compounding short fibres with $CaO-P_2O_5-SiO_2-Al_2O_3$ glass. Biomaterials, 2000, 21(20): 2051-2058.

[41] Matkó S, Anna P, Marosi G, Szep A, Keszei S, Czigany T, Pölöskei K. Use of reactive surfactants in basalt fiber reinforced polypropylene composites//Macromolecular Symposia. Weinheim: WILEY-VCH Verlag, 2003, 202(1): 255-268.

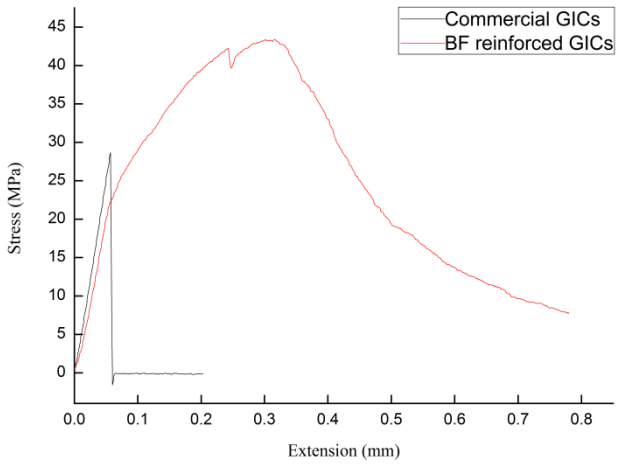

Figure 1. Stress-extension curves of commercial GICs and BF reinforced GICs obtained from three-point bending test.

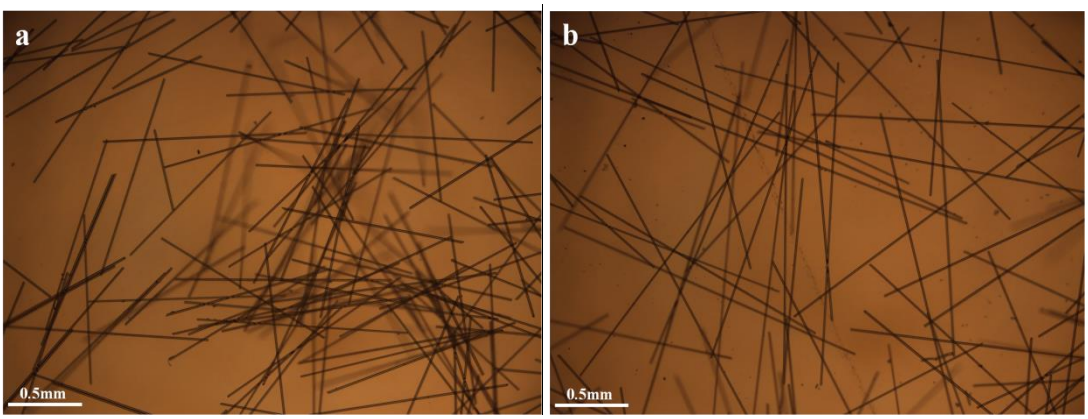

Figure 2. Microscope photos of basalt fibers: (a) 1 mm basalt fibers; (b) 2 mm basalt fibers

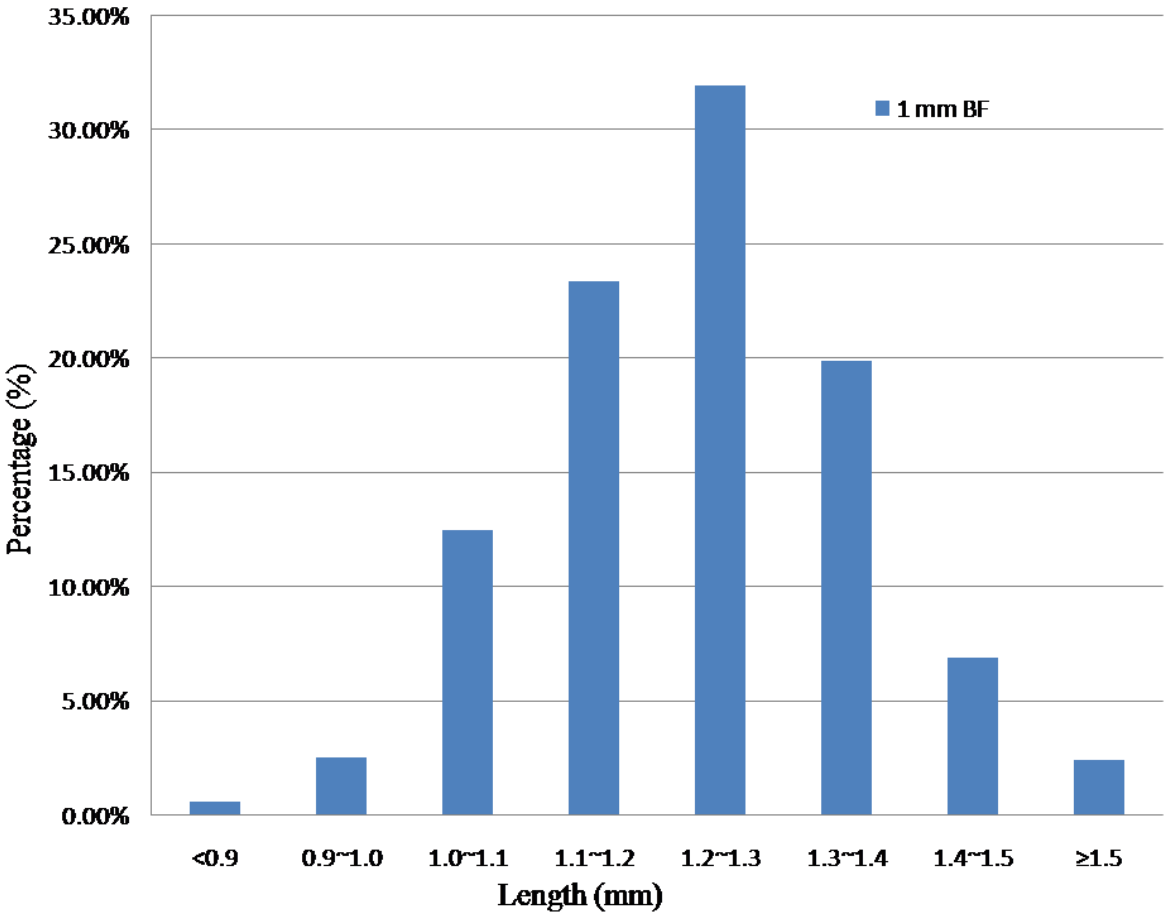

Figure 3. Length distribution of 1 mm basalt fibers.

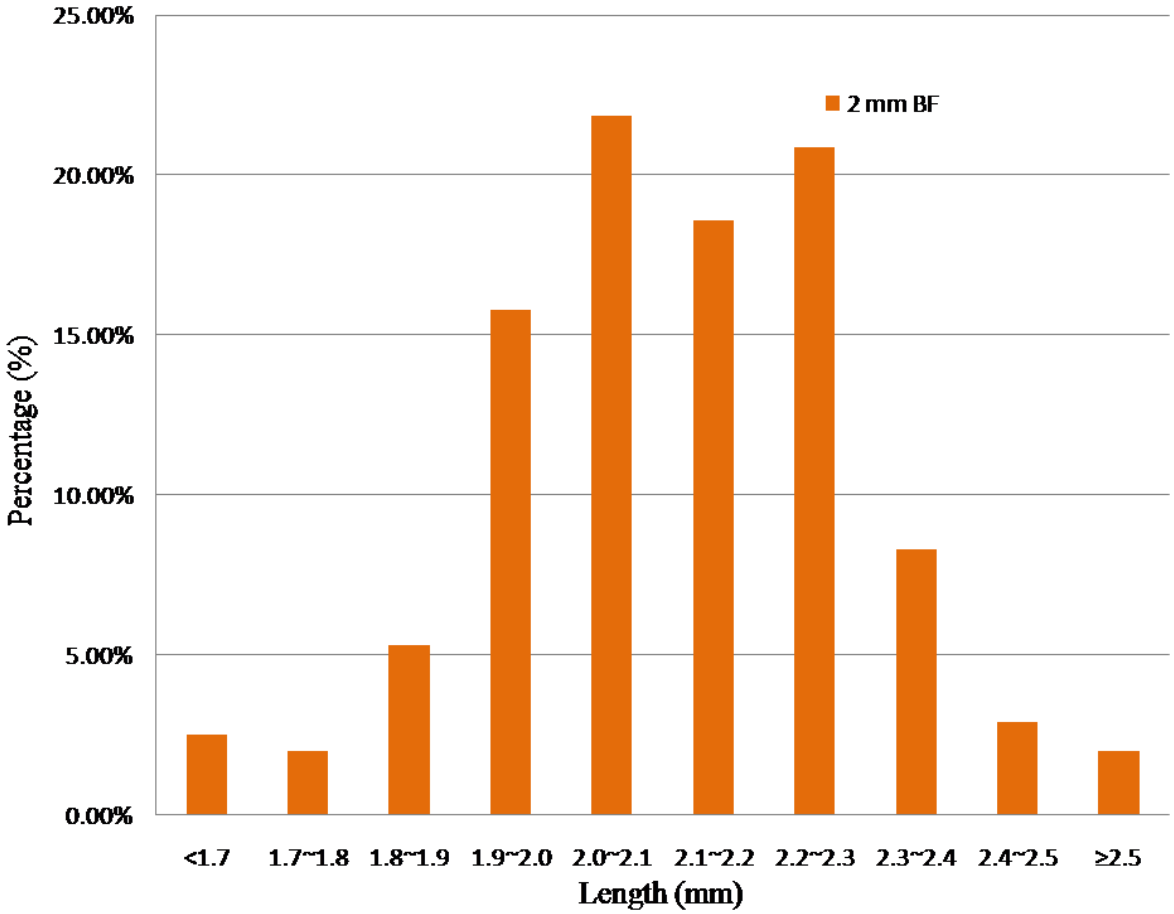

Figure 4. Length distribution of 2 mm basalt fibers

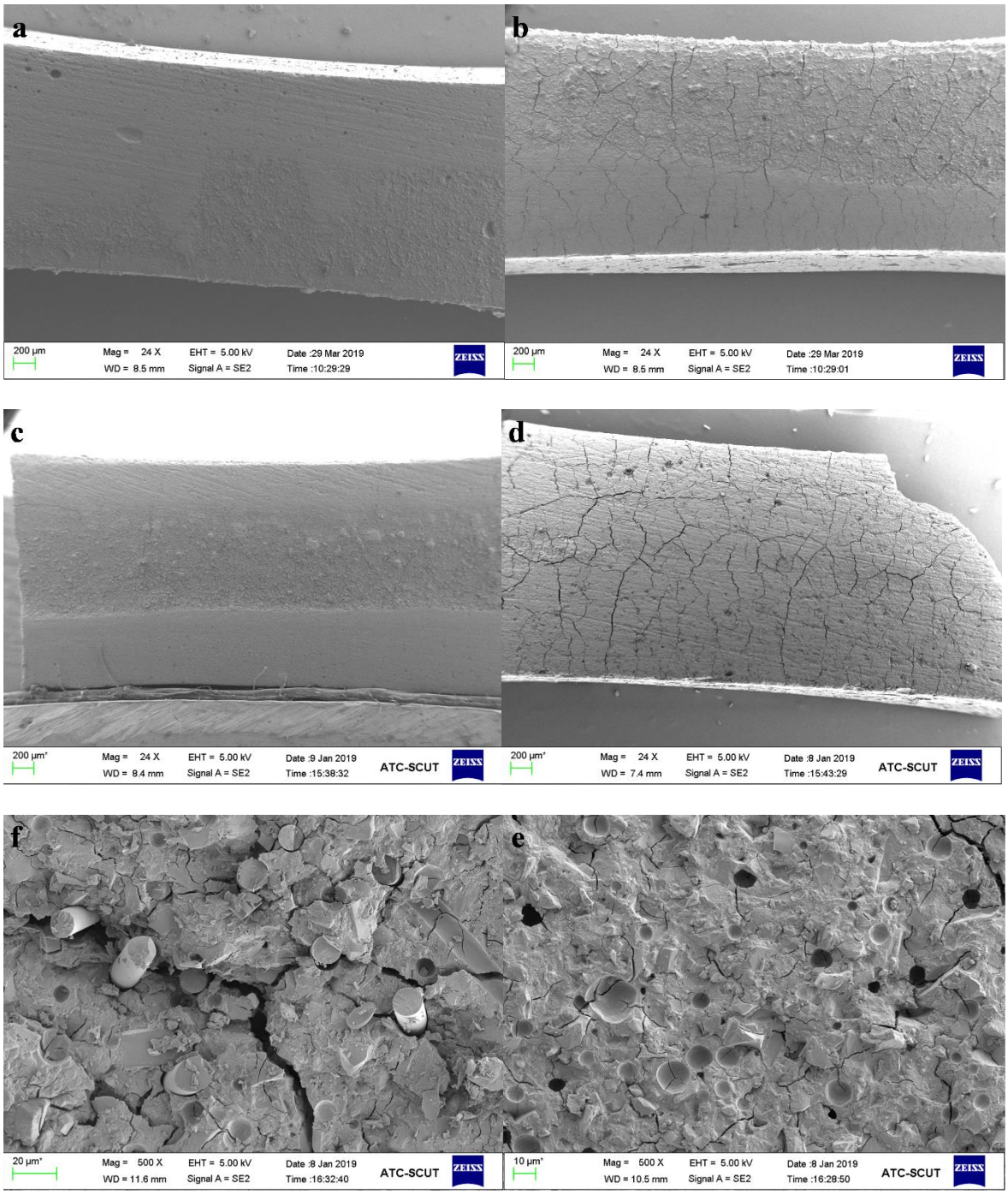

Figure 5. SEM photos of fracture surface and side surface of tested three-point bending specimens that immersed in deionized water for 24 hours: (a) side surface of control GIC after three point bending test; (b) side surface of BF reinforced GIC after three point bending test; (c) side surface of control GIC before three point bending test; (d) side surface of BF reinforced GIC before three point bending test; (e) fracture surface of control GIC; (f) fracture surface of BF reinforced GIC.

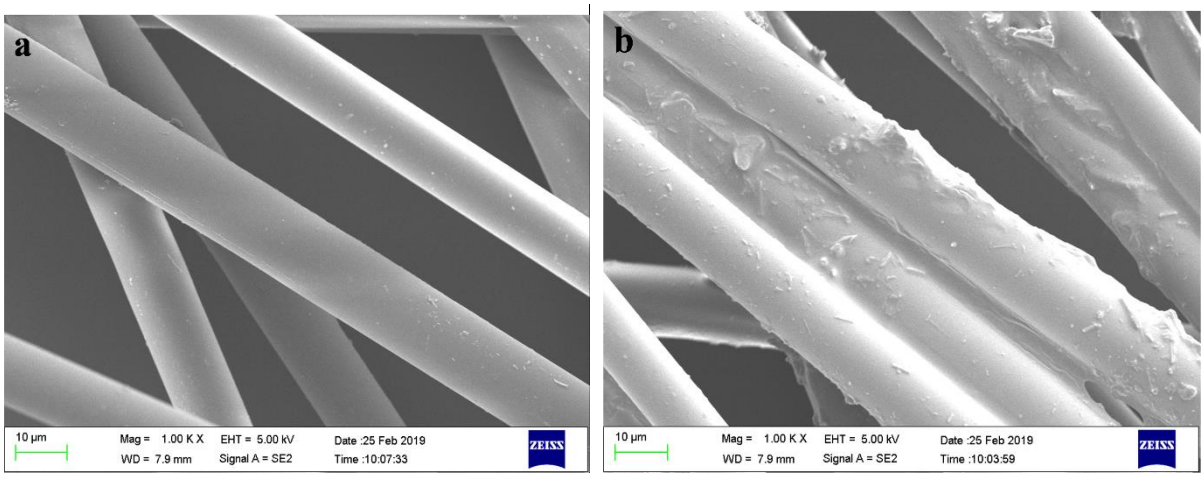

Figure 6. SEM photos of BF: (a) BF without cement liquid treatment mixing; (b) BF treated with cement liquid.